We are IntechOpen, the world's leading publisher of Open Access books
Built by scientists, for scientists

6,900
Open access books available

185,000
International authors and editors

200M
Downloads

154
Countries delivered to

Our authors are among the

TOP 1%
most cited scientists

12.2%
Contributors from top 500 universities

WEB OF SCIENCE™

Selection of our books indexed in the Book Citation Index
in Web of Science™ Core Collection (BKCI)

Interested in publishing with us?
Contact book.department@intechopen.com

Numbers displayed above are based on latest data collected.
For more information visit www.intechopen.com

Kinetic Energy Harvesting

Helios Vocca and Francesco Cottone

Additional information is available at the end of the chapter

1. Introduction

The recovery of wasted energy present in the ambient that is a reject of artificial or natural processes to power wireless electronics is paving the way for enabling a huge number of applications. One of the main targeted technologies that meets the levels of harvestable power, typically few hundreds of microwatts, is represented by wireless sensor networks (WSNs) [1]. This technology consists of a grid of spatially-distributed wireless nodes that sense and communicate information like acceleration, temperature, pressure, toxicity of the air, biological parameters, magnetic field, light intensity and so on, among each other and up to the end user through a fixed server. In the next years, WSNs will be massively employed in a wide range of applications such as structural monitoring, industrial sensing, remote healthcare, military equipment, surveillance, logistic tracking and automotive monitoring. In fact, harvesting energy directly from the ambient not only represents a realistic mean to integrate or substitute batteries, but is the sole way for enabling many contemporary and future wireless applications that will be all integrated in the so called "internet of things" [2].

Actually, WSNs already have the characteristics of ubiquity, self-organizing and self-healing but they would not be deployable unless they will also be self-powering. As a matter of fact, it is very expensive and impractical to change batteries in most of the anticipated potential applications. For long-term operation in inaccessible or harsh locations, energy harvesting is a key solution. For example, long-term environmental, structural health of buildings or bridge monitoring and control would require many thousands of integrated sensors impossible to be replaced or maintained. The possibility for chronically ill patients to be continuously monitored without changing batteries would represent a significant improvement in their life quality.

Among various renewable energy present in the environment such as solar, radio frequency RF, temperature difference and biochemical, kinetic energy in the form of mechanical vibra-

tions is deemed to be the most attractive, in the low-power electronic domain, for its power density, versatility and abundance [3]. This type of energy source is located in buildings, vibrating machineries, transportations, ocean waves and human beings, and it can be converted to power mobile devices.

The power consumption of wireless sensors has been largely reduced in the last years thanks to the Ultra-Low-Power electronics [4]. Typical power needs of mobile devices can range from few microwatts for wristwatches, RFID, MEMS sensors and actuators up to hundreds of milliwatts for MP3, mobile phone and GPS applications. They are usually in a sleep state for the 99.9% of their operation time, waking up for a few milliseconds only to communicate data. Consequently, their average power consumption has been reduced below 10μW in order to match the power density capability of current generators (100-300 microwatts per cubic centimeter). For comparison, a lithium battery can provide 30μW/cc for 1 year or 30mW/cc for just 10 hours, while a vibration-driven generator could last for at least 50 years with the same power level [5]. Along with virtually infinite operational life, many other benefits come from motion-driven energy harvesting: no chemical disposal, zero wiring cost, maintenance-free, no charging points, capability for deployment in dangerous and inaccessible sites, low cost of retrofitting, inherent safety and high reliability.

A typical integrated vibration-powered wireless sensor includes an embedded vibration energy harvester (VEH), multiple-sensor module, microcontroller and a transceiver (Figure 1). Due to the variable nature of vibrations in their intensity and frequency, the device also contains an AC/DC voltage regulation circuit, which in turn can recharge a temporary storage system, typically a super-capacitor or a thin film Lithium battery. Capacitors are usually preferred as temporary storage systems for their longer lifetime, higher power density and fast recharging. In some applications, however, a storage system is not even necessary. The vibration energy harvester module is often tailored for the specific application and vibration spectrum of the source: harmonic excitation, random noise or pulsed movement.

2. Main conversion techniques

There are three main categories of kinetic-to-electrical energy conversion systems: piezoelectric, electrostatic and electromagnetic. In addition, there is the magnetostrictive branch as a variant of piezoelectric except for the use of magnetically polarized materials [6]. Each technique presents advantages and drawbacks. Therefore, there not exist a technique suitable for all cases and the optimal choice depends on the specific application.

Piezoelectric transducers make use of electrically polarized materials such as Barium Titanate (BaTiO3), Zinc Oxide (ZnO) and Lead Zirconate Titanate ($Pb[Zr_xTi_{1-x}]O_3$), commonly known as PZT which is considered one of the best materials for high electromechanical coupling. The direct piezoelectric effect used for energy harvesting was early discovered by French physicists Jacques and Pierre Curie in 1880. It occurs when an electric charge is generated within a material in response to applied mechanical stress (Figure 2). The strain and coupling coefficients in the fundamental piezoelectric equations are in general much higher in 33 mode than
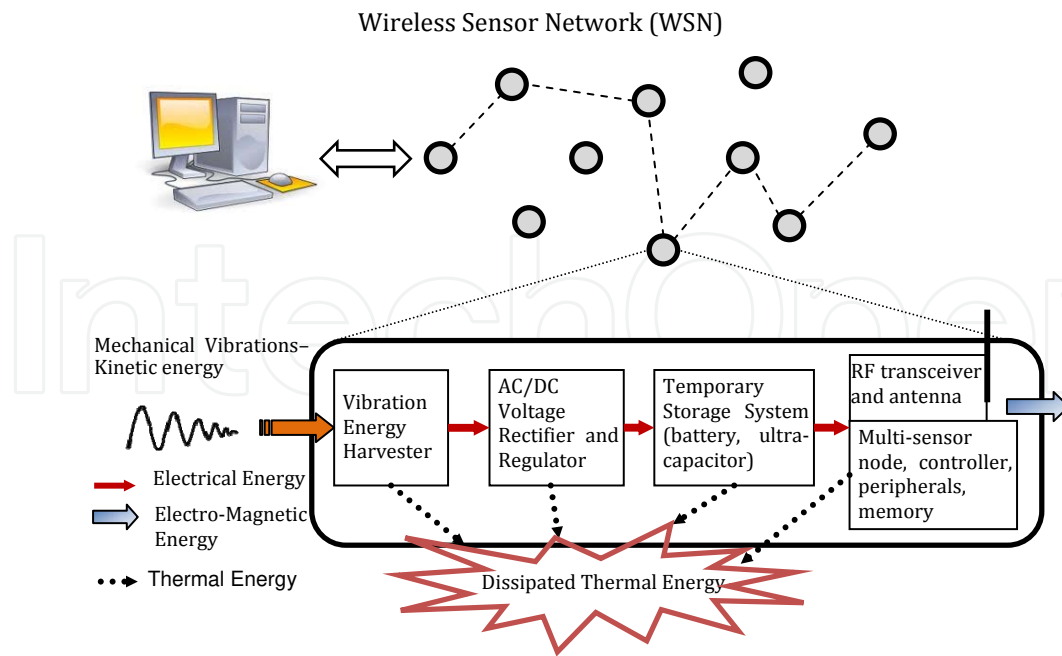
Figure 1. Wireless sensor network and vibration-driven wireless node with power fluxes.

in 31 [7]. However the 33 mode of bulk crystal corresponds to very high natural frequencies (~1 to 100 kHz), while longitudinal strain is easily produced within a cantilever beam that resonates at lower frequencies (~100 Hz) (Figure 2c).
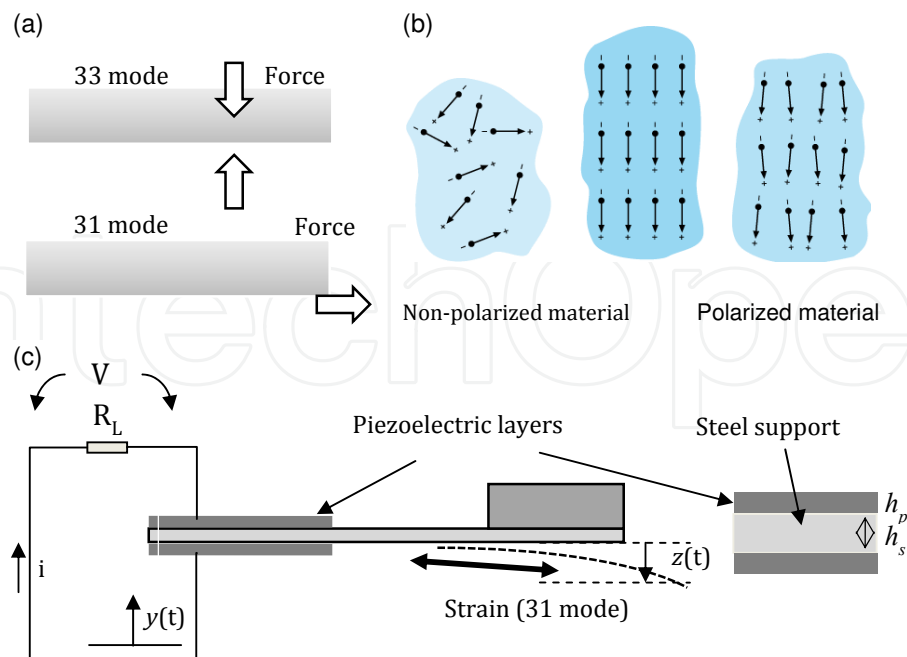

Figure 2. (a) Direct piezoelectric effect with 33 and 31 strain-charge coupling. (b) Polarization process scheme. (c) Drawing of bimorph piezoelectric cantilever beam.

Piezoelectric systems are capable of high voltage level (from 2 to several volts), well adapted for compact size and very good in terms power density per unit of volume. However, piezoelectric coupling decreases very fast at micrometric scale and relatively large load impedances are required to reach the optimal working point [8]. Besides, other problems must be considered such as aging, depolarization and brittleness. For low frequency applications, like those related to wearable sensors, polymer-based materials (e.g. dielectric elastomers) constitute a valid alternative to ceramics because of their flexibility, inexpensiveness and durability [9].

Electromagnetic technique is simply realized, according to Faraday's law, by coupling a static magnetic field produced by a permanent magnet and a solenoid in relative motion – one of which usually acts as a stator; the other as a mover. These systems show complementary behaviour in terms of frequency bandwidth and optimal load in relation to piezoelectric techniques. They are recommended for lower frequencies (2-20 Hz), small impedance and medium size [10]. Furthermore, their cost is smaller than other solutions. Most of the commercial solutions are available at centimetre scales because they exhibit higher power density than piezoelectric devices. On the other hand, the integration of electromagnetic harvesters into micro-electro-mechanical-systems (MEMS) results difficult. However, some of these limitations have been overcome to date [11-13].
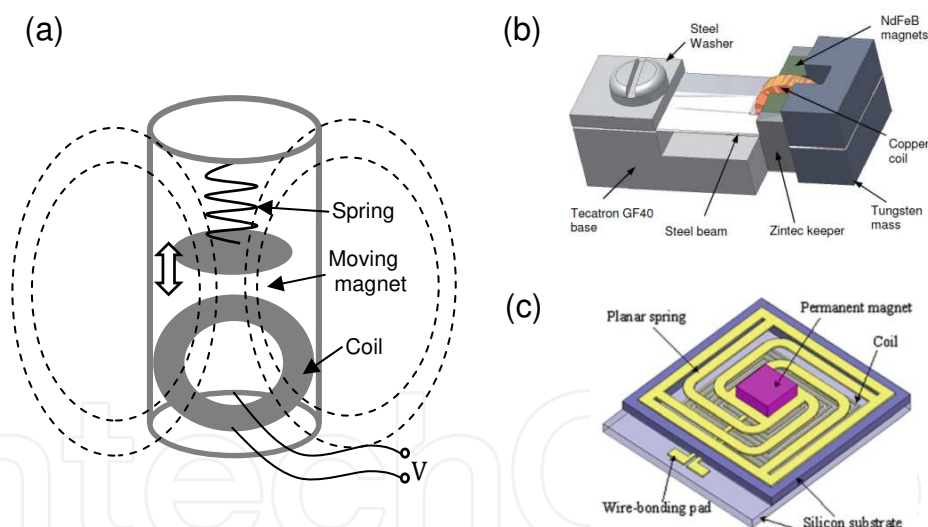

Figure 3. (a) Simple architecture of em-VEH where a moving magnet (mover) oscillates with respect to a fixed coil (stator). (b) Moving magnet across coil arrangement with discrete components [11-13]. (c) Microfabricated em-VEH where a small magnet oscillates towards a planar coil [11].

Electrostatic harvesters basically consist of a variable capacitor in which one electrode is attached to an oscillating mass suspended by beams and the counter electrode is fixed elsewhere in the support structure. When a force is applied to the mass either the dielectric gap or the overlap surface of electrodes varies depending on the moving direction: the first case being referred to as an in-plane gap-closing converter (Figure 4a), while the second case as an overlap varying converter (Figure 4b). As a consequence, the capacitance changes and

additional charges occur at the electrodes in order to balance the bias voltage. Hence, during the movement of the proof mass, a current flows through a load shunted to plates. A similar method of fixed bias voltage is that of charge constrained where a constant charge is held into the plates by means of a battery or another capacitor.

One of the main disadvantages of electrostatic vibration harvesters is the need of an external voltage source in order to be pre-charged. This fact seems to contrast with the goal of energy recycling from the ambient, but makes sense if the source comes from the energy storage associated to the harvester [12]. In that case the generator only needs to be kick-started at the beginning of the conversion process. Some designs overcome this problem by using electrets to provide the pre-charge bias voltage [14].
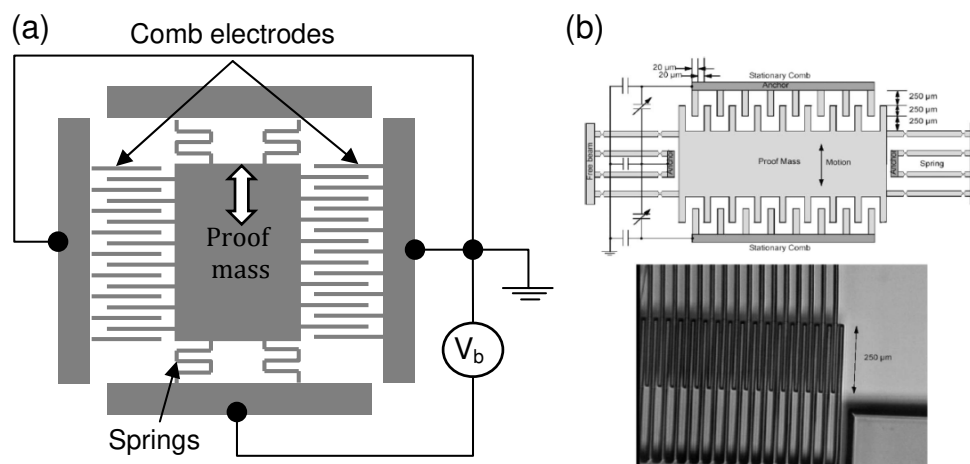

Figure 4. (a) Schematic of comb gap-closing electrostatic VEH. (b) Example of MEMS in-plane overlap electrostatic VEH [15].

Nevertheless, electrostatic technology is very well suited for MEMS manufacturing as employs the same elements of micro accelerometers [14]. Moreover, the silicon based MEMS do not have problems of aging as for piezoelectric materials. However the generated power is pretty much small compared to piezoelectric and electromagnetic [16].

Nowadays, vibration energy harvesters are delivered on the real market by some leading companies such as Perpetuum Ltd, Ferro Solution and Mide Volture although they have quite bulky size. The power density of commercial harvesters ranges from 10 to 300μW/cc relative to acceleration levels of 0.01-1g rms. Prototypes of MEMS-based harvesters have been demonstrated by universities and private teams, though they are still at experimental stage. Beeby et al. have implemented a vibration-powered wireless sensor node with embedded micro-electromagnetic generator [3]. Millimetre-sized electrostatic generators were formerly realized by Roundy et al. [11]. Miao implemented a parametric generator for biomedical applications [17] and examples of piezoelectric nano-mechanical generators are also emerging [18]. Mahmood and Basset have successfully built and tested an efficient MEMS-based electrostatic harvester [19, 20].
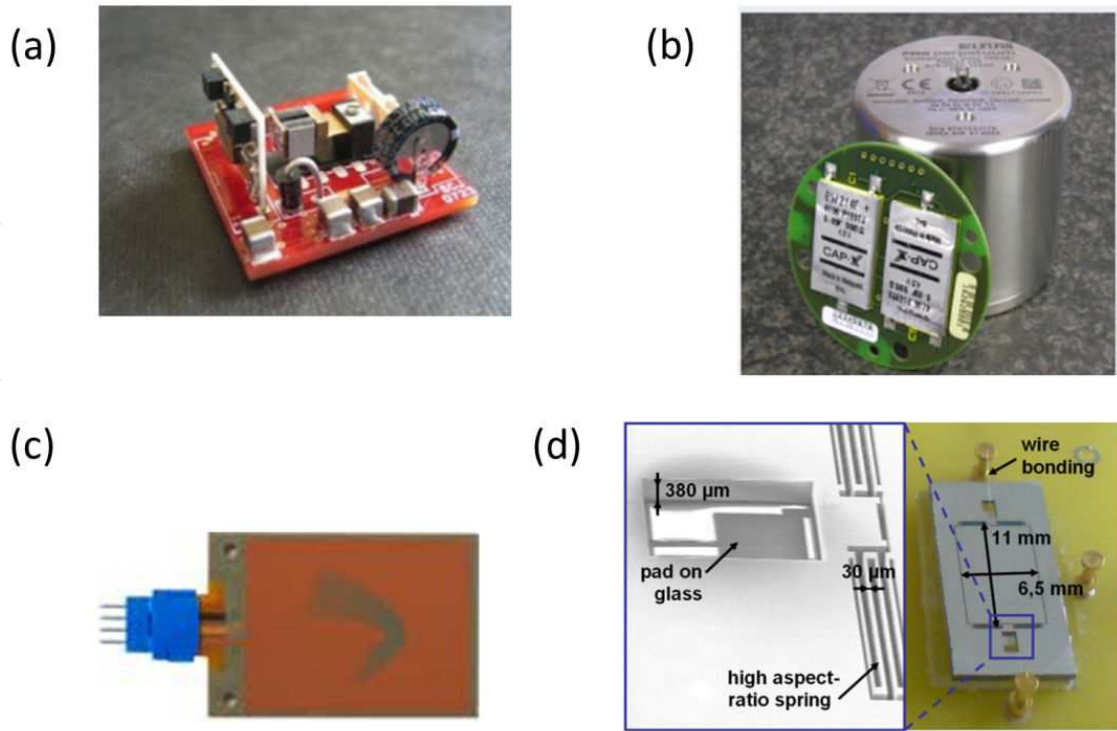
Figure 5. Examples of micro vibration energy harvester: (a) electromagentic [16] and (b) (Perpetuum), (c) piezoelectric (Midé), (d) electrostatic [11].

3. Linear spring-mass-damper models of VEHs

Kinetic energy harvesters are divided into two categories: those that utilize direct application of force and those that make use of the inertial force associated to a moving mass m. Inertial generators, are preferred to direct-force devices for vibration energy harvesting as they only need one point of attachment to a vibrating structure, thus allowing a simpler miniaturization.

Figure 6 illustrates basic models of (a) direct and (b) inertial force vibration-based generators independent from the conversion technology. In the second case, the driving force $F(t)$ is equal to $-m\ddot{y}$, where the base vibrations are represented as $y(t)$ and dot stands for the derivative with respect to time. $z(t)$ is the relative motion between the housing and proof mass, k is the spring stiffness, d is the parasitic damping, f_e represents the electrical restoring force due to the transduction mechanism. Finally, the electrical part includes the resistive load R_L through which flows the generated current i.

Williams and Yates early defined a basic technology independent model of micro-electric generator for vibration energy harvesting [16]. In that case the conversion force f_e being considered as an electrical damping force proportional to the velocity $f_e = -d_e\dot{z}$. However, the electrical restoring force can in general be a complex function of the mass displacement, velocity and acceleration. In addition, such an approximation does not take into account of the effect of the electrical branch coupled to the mechanical system.
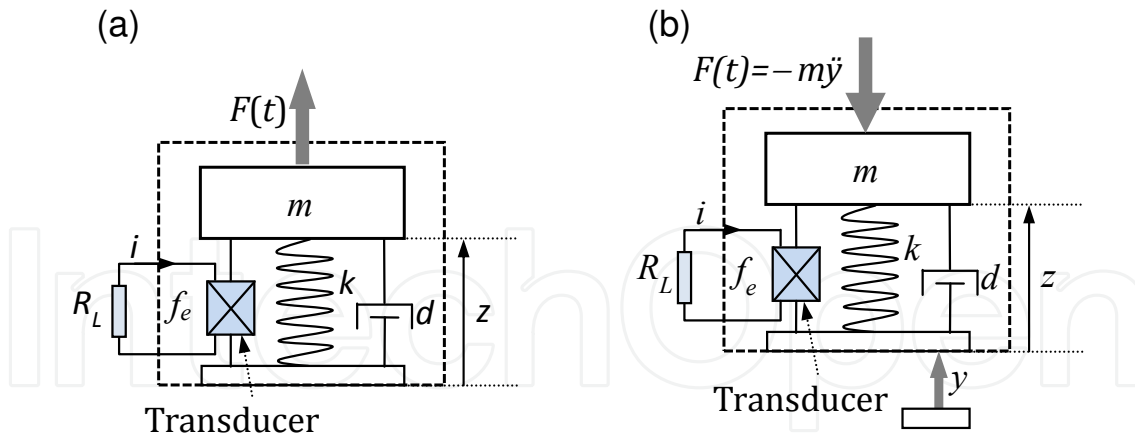
Figure 6. Models of non-technology specific (a) direct-force and (b) inertial-force generators. The electrical force f_e can be in general a complicated function of displacement, velocity or acceleration.

In the following we describe the lumped parameters model of the VEH by including the electrical domain as sketched in Figure 6b. This can be then applied to different types of linear conversion systems. The coupled governing equations of a generic 1-DOF vibration-driven generator are derived by the second Newton's law and Kirchhoff's law as follows

$$m\ddot{z} + d\dot{z} + kz + \alpha V = -m\ddot{y}, \tag{1}$$

$$\dot{V} + (\omega_c + \omega_i)V = \omega_c \lambda \dot{z}, \tag{2}$$

where dots stand for time-derivatives. The first equation describes the dynamics of the inertial mass while the second equation accounts for the coupled electrical circuit. V is the produced voltage across the electrical resistance and α is the electromechanical coupling factor; ω_c represents the characteristic cut-off frequencies of the electrical circuit of the system operating as high-pass filter due to the specific transduction technique. This parameter is the inverse to the characteristic time τ of the electrical branch, that is $\omega_c = 1/\tau$. ω_i has the same meaning but corresponding to the internal resistance R_i of the system. Finally, λ is the electromechanical conversion factor. These characteristic parameters are derived from the harvester design depending on the specific conversion method and architecture as explained in the following examples. Hereafter we will only treat the piezoelectric and electromagnetic case, as the electrostatic is inherently nonlinear when considering the electrical force between close electrostatic plates.

3.1. Case 1: piezoelectric cantilever generator

Starting by the constitutive piezoelectric equations [21], for a bimorph piezoelectric cantilever like the one shown in Figure 2c with active layers wired in parallel, the above characteristic parameters are derived

$$\alpha = kd_{31} / h_p k_2, \qquad \text{(a)} \qquad \lambda = \alpha R_L, \qquad \text{(b)}$$
$$\omega_c = 1 / R_L C_p, \qquad \text{(c)} \qquad \omega_i = 1 / R_i C_p, \qquad \text{(d)}$$

<div align="right">(3)</div>

where h_P and h_s are the thickness of piezoelectric and support layer respectively; d_{31}, E_p, ε_0, ε_r and C_p are the piezoelectric strain factor, Young's modulus, vacuum and relative dielectric permittivity and, finally, the equivalent capacitance of piezoelectric beam. These constants are related to the following structural parameters as derived in [7]

$$k = k_1 k_2 E_p, \qquad \text{(a)}$$

$$k_1 = \frac{2I}{b(2l_b + l_m - l_e)}, \qquad \text{(b)} \qquad k_2 = \frac{3b(2l_b + l_m - l_e)}{l_b^2 \left(2l_b + \dfrac{3}{2} l_m\right)}, \qquad \text{(c)}$$

$$b = \frac{h_s + h_p}{2}, \qquad \text{(d)} \qquad I = 2 \left[\frac{w_b h_p^3}{12} + w_b h_p b^2 \right] + \frac{E_s / E_p w_b h_s^3}{12}, \qquad \text{(e)}$$

<div align="right">(4)</div>

where k represents the effective elastic stiffness, k_1 and k_2 are the average strain to mass displacement and the input force to average induced stress, b is a geometrical parameter of the bimorph structure and I is the composite inertial moment of the beam. Usually, the internal resistance R_i of a piezoelectric crystal is very high, hence ω_i is negligible.

3.2. Case 2: electromagnetic generator

Let consider a simple "magnet in-line coil" electromagnetic generator as schematized in Figure 3a. we can rewrite the characteristic parameters as

$$\alpha = Bl / R_L, \qquad \text{(a)} \qquad \lambda = Bl = \alpha R_L, \qquad \text{(b)}$$
$$\omega_c = R_L / L_e, \qquad \text{(c)} \qquad \omega_i = R_i / L_e, \qquad \text{(d)}$$

<div align="right">(5)</div>

with B representing the magnetic field across the coil of total length l and self-inductance L_e. Even in this case, by assuming an internal resistance of the coil R_0 small with respect to the external load ($R_0 \ll R_L$), we can neglect ω_i. Actually, the above fundamental parameters are also valid for other systems such as "magnet across coil" arrangement depicted in Figure 3b.

In both cases the governing equations are the same, and they can be also rewritten in a more convenient nondimensional form similar to [22].

3.3. Transfer functions

Let now consider the simple case of harmonic excitation $\ddot{y}(t) = Y_0 e^{j\omega t}$ as input. We can transform the motion equations(1) and (2) into the Laplace domain, with $s = j\omega$ as the Laplace variable (where j stands for the imaginary unit). The function $Y(s)$, $Z(s)$, and $V(s)$ are the acceleration

amplitude, mass displacement and output voltage delivered to the resistive load respectively. Thus, the governing equations for the single-mass generator can be rewritten as the system

$$
\begin{pmatrix} ms^2 + ds + k & \alpha \\ -\lambda\omega_c s & s + \omega_c \end{pmatrix} \begin{pmatrix} Z \\ V \end{pmatrix} = \begin{pmatrix} -mY \\ 0 \end{pmatrix}
\tag{6}
$$

the left-side matrix, that we can name A, represents the generalized impedance of the oscillating system. By means of linear algebraic methods we can easily solve the above system equation, so that the displacement $Z(s)$ and output voltage $V(s)$ are given by

$$
Z = \frac{-mY}{\det A}(s + \omega_c) = \frac{-mY \cdot (s + \omega_c)}{ms^3 + (m\omega_c + d)s^2 + (k + \alpha\lambda\omega_c + d\omega_c)s + k\omega_c},
\tag{7}
$$

$$
V = \frac{-mY}{\det A}\lambda\omega_c s = \frac{-mY \cdot \lambda\omega_c s}{ms^3 + (m\omega_c + d)s^2 + (k + \alpha\lambda\omega_c + d\omega_c)s + k\omega_c}.
\tag{8}
$$

Hence, the transfer functions between displacement and voltage over input acceleration are therefore given by

$$
H_{ZY}(s) = \frac{Z}{Y}, \quad \text{(a)} \qquad H_{VY}(s) = \frac{V}{Y}. \quad \text{(b)}
\tag{9}
$$

By substituting $s=j\omega$ in (8), we can calculate the electrical power dissipated across the resistive load

$$
P_e(\omega) = \frac{|V(j\omega)|^2}{2R_L} = \frac{|H_{VY}(j\omega)|^2 |Y(j\omega)|^2}{2R_L} =
$$
$$
= \frac{Y_0^2}{2R_L}\left| \frac{-m\lambda\omega_c j\omega}{(\omega_c + j\omega)(-m\omega^2 + j\omega d + k) + \alpha\lambda\omega_c j\omega} \right|^2.
\tag{10}
$$

By introducing the natural frequency of the undamped oscillation $\omega_n = \sqrt{k/m}$ and the normalized damping factor $\zeta = d/2m\omega_n$ into the above equation, it becomes

$$
P_e(\omega) = \frac{Y_0^2}{2R_L}\left| \frac{-\lambda\omega_c j\omega}{(\omega_c + j\omega)(\omega_n^2 - \omega^2 + 2\zeta\omega_n j\omega) + \alpha\lambda\omega_c j\omega/m} \right|^2
\tag{11}
$$

In Figure 7 the graph of the normalized power function over the nondimensional variable ω/ω_n of a generic vibration-based generator is shown.
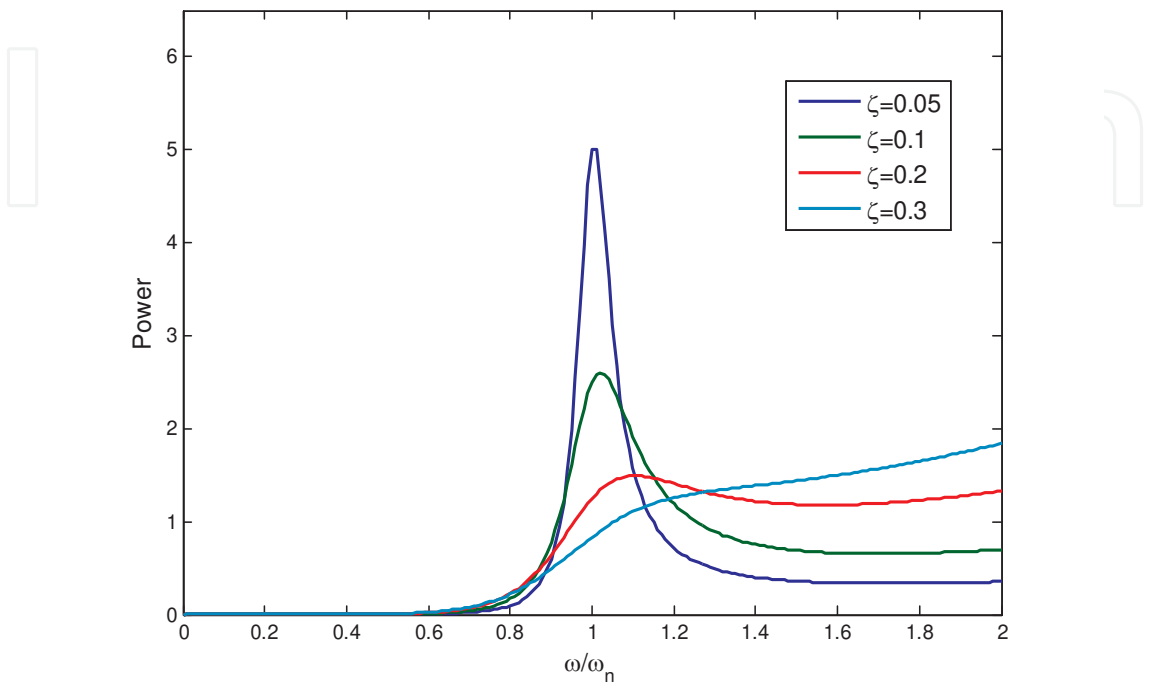

Figure 7. Normalized power function of a generic vibration-base harvester.

The main limits of a linear vibration energy harvester include:

• narrow bandwidth, that also implies applications with vibrating sources tuned around resonant frequency of the harvester,

• versatility and adaptation to variable spectrum vibration sources,

• at MEMS scale: small inertial mass and maximum displacement, limited power not suitable for milliwatts electronics (10-100mW).

In any case, for applications and environments that feature a vibration source consistent in frequency and time, linear systems can still represent an optimal choice.

4. Beyond linear energy harvesting

In most of the reported studies, the energy harvesters are designed as linear oscillators that match their resonant frequencies to the excitation frequencies of the environment to achieve the maximum output power.

This condition can be easily performed when the excitation frequency is well known and stable in time. It is in fact possible to choose the correct geometry and harvester dimension for

frequency matching. However, when the ambient excitation frequency is unknown or varies in time, the previous conditions are not guaranteed. Therefore a harvester with a fixed resonant frequency is not able to achieve an optimal output power.

Various strategies have been investigated to overcome this practical inconvenient and increase the bandwidth of vibration-based harvesters. In the following the state-of-the-art techniques are summarised in three main categories: resonance frequency tuning, multimodal oscillators and frequency up-conversion. A complete technique review is presented by [23].

4.1. Frequency tuning

In some cases it has been demonstrated [24] that the resonance frequency of an oscillator can be tuned to the main exciting frequency in two different ways: passive and active. The passive mode requires an intermittent power input (manual or automatic) to check and tune the system until the frequency match is complete, then the power requirement is zero since the excitation frequency varies again. The active mode is more power demanding since a continuous power is needed to tune the system; this higher power consumption brings the effect to increase the harvester efficiency.

The tuning mechanisms can be realised mechanically using springs or screws, with magnets or using a piezoelectric material.

Few works have been presented in the last years showing possible manual parameter adjustments to change the harvester stiffness or its mass configuration. The oscillator stiffness is changed with a pre-loaded or a pre-deflected, performing a softening or a hardening of the system.
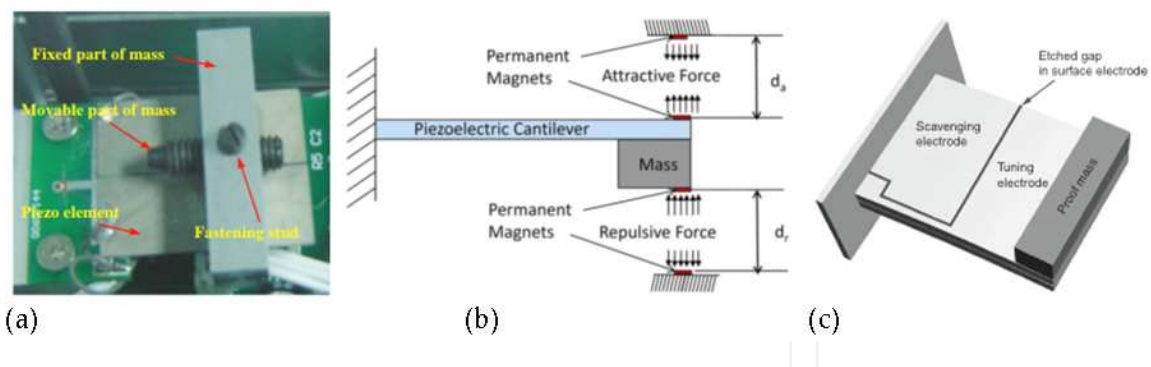

Figure 8. Three tunable vibration-based solutions: (a) Piezoelectric cantilever with a movable mass (source: Wu et al. 2008 [25]), (b) Piezoelectric cantilever with magnetic tuning (source: Challa et al. 2008 [26]), (c) Piezoelectric beam with a scavenging and a tuning part (source: Roundy and Zhang 2005 [27]).

In Figure 8 three tunable solutions are presented. The three harvesters are realized with a piezoelectric beam, in which the tuning mechanism is purely mechanical in the first case by [25], magnetic in the second by [26], and piezoelectric in the third by [27].

The solution (a) is realized with a proof mass consisting in a fixed part combined with a movable part. The gravity centre of the proof mass can be adjusted by driving the screw. The

fixed part of the mass is made with a relatively small density material and the tuning mass with a higher density one. In this way the frequency tunability is increased by moving the distance of the centre of gravity of the proof mass. In this prototype, the frequency range can be manually varied in the 130-180 Hz range moving the tip mass up to 21 mm.

The solution (b) of Figure 8 is realized by coupling two magnets fixed to the free end of the cantilever beam to two other magnets fixed to the top and bottom sides of the enclosure device. All the magnets have a vertical magnetization in such a way to perform an attractive and repulsive force on each side of the beam. Manually tuning the distance between the magnets using a screw, the magnetic force can be changed inducing a change in the cantilever stiffness. The resonant frequency can be varied in the 22-32 Hz range.

The latter case (c), of Figure 8, presented by Roundy and Zhang [25], is an active tuning mechanism. The electrode was etched to create both scavenging and tuning parts on the same beam. They analytically demonstrated that an active tuning actuator never resulted in a net increase in power output. This is explained because the power required to continuously tune the beam resonant frequency exceeds the harvested power increase.

Table 1, taken from Tang et al.[25], summarizes various tuning methods.

Author	Methods	Tuning range (Hz)	Tunability, $\left(\frac{\text{frequency change}}{\text{average frequency}}\right)$ (%)	Tuning load (force, distance, and voltage)	Energy or power for tuning	Automatic controller
Leland and Wright (2006)	Mechanical (passive)	200–250 (7.1 g tip mass)	22.22	Up to 65 N	−	×
Eichhorn et al. (2008)	Mechanical (passive)	292–380	26.19	Up to 22.75 N	−	×
Hu et al. (2007)	Mechanical (passive)	58.1–169.4	97.85	−50–50 N	−	×
Morris et al. (2008)	Mechanical (passive)	80–235 (can be wider)	≥98.41	≈1.25 mm	−	×
Loverich et al. (2008)	Mechanical (passive)	56–62	10.17	0.5 mm	−	×
Wu et al. (2008)	Mechanical (passive)	130–180	32.26	21 mm	−	×
Challa et al. (2008)	Magnetic (passive)	22–32	37.04	3 cm	85 mJ	×
Reissman et al. (2009)	Magnetic (passive)	88–99.38	12.15	1.5 cm	−	×
Zhu et al. (2008)	Magnetic (passive)	67.6–98	36.71	3.8 mm	2.04 mJ/mm	√
Wu et al. (2006)	Piezoelectric (active)	91.5–94.5	3.23	−	μW level (for controller)	√
Peters et al. (2009)	Piezoelectric (active)	66–89 (actuator PL140)	29.68	±5 V	150 mW (discrete control circuit)	√
Roundy and Zhang (2005)	Piezoelectric (active)	64.5–67	3.80	5 V	440 μW	×
Wischke et al. (2010)	Piezoelectric (semi-passive)	20 (10 mm long electrode)	≈6.7	−65 to +130 V	200 μJ	×

Table 1. Summary of various resonance tuning methods (source: Tang et al. 2010 [24]).

4.2. Multimodal energy harvesting

The multimodal approach consists in a multi-vibration harvester, designed to be excited when the natural driving frequency approaches one natural frequency of the harvester. In this case

useful power can be harvested over multiple frequency spectra, increasing the bandwidth that can be covered for efficient energy harvesting.

One way to design a multimodal VEH consists in the combination of more transduction mechanisms together. In [24] a hybrid scenario was presented by Tadesse et al. as shown in Figure 9a. The harvester consists of a cantilever beam with piezoelectric crystal plates bonded on it at a fixed distance each other; a permanent magnet is attached at the cantilever tip oscillating within a coil fixed to the housing structure. It this configuration the electromagnetic transducer generates high output power at the cantilever first mode (at 20 Hz), while the piezoelectric transducer generates higher power at the cantilever second mode (at 300 Hz). The combination of the two schemes in one device is able to improve significantly the harvester response covering two frequency ranges. The drawback of this solution is the difficulty in combining the output power from two different mechanisms, thus requiring two separate converting circuits.

A different approach rather than exploiting the energy present at different modes of a single oscillator is to design a cantilever array integrated in one single device. If the geometric parameters of the harvester are appropriately selected, a wide vibration bandwidth can be exploited. In Figure 9b and 9c two different array solutions are presented.
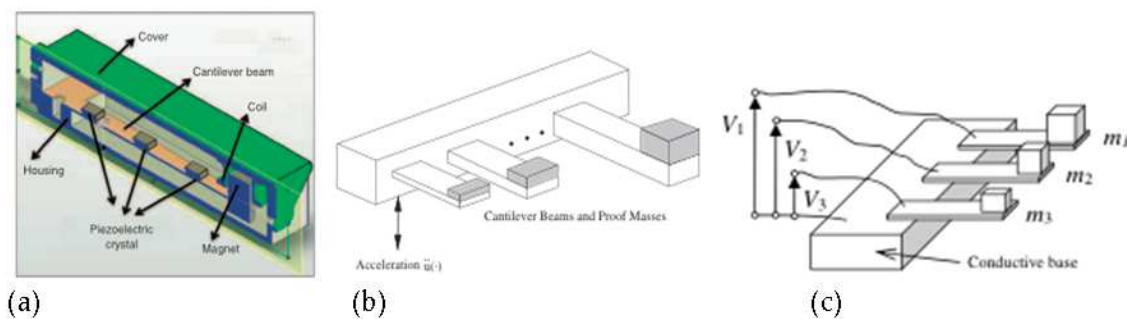

Figure 9. Multimodal VEH schematics. (a) Hybrid harvester with piezoelectric and electromagnetic transduction mechanisms (source: Tadesse et al. 2009 [28]). Piezoelectric cantilever arrays with various lengths and tip masses (b) (source: Shahruz 2006 [28]) and same cantilevers with different tip masses (c) (source: Ferrari et al. 2008 [29]).

In the first design, (b), various cantilevers with different lengths and tip masses attached to a common base compose a piezoelectric cantilever array. In the second, (c), the cantilevers are the same but the first mode response is changed varying the tip masses. Each cantilever presents a unique resonant frequency, the combination of which into a single device creates a sort of mechanical band-pass filter. By properly selecting the different parameters, the device can be designed to provide a voltage response on a wide frequency range.

It has been demonstrated by [30] that the improved bandwidth and performance were worth the modest increase in size of the proposed array device. A cantilever array configuration in respect to the hybrid solution, doesn't present the difficulty in combining the output power from the different mechanisms, but requires one rectifier for each cantilever to avoid output cancellation due to the phase difference between the cantilevers.

As a matter of fact, the multimodal approach increases the bandwidth increasing the volume or the weight of the harvester, thus reducing the energy density. Specifically for the cantilever array, only one cantilever or a subset of them are active at the same time generating a certain amount of power while the others are at off-resonance. Hence, knowing the dominant spectrum of the ambient vibrations, the harvester has to be carefully designed to prevent a dramatic efficiency loss.

4.3. Up-conversion energy harvesting

In many practical situations, the ambient vibrations suitable for energy harvesting including human vibrations, natural events (i.e. wind, seismic motion), common household goods (i.e. fans, fridges, washing machine), automobiles, airplanes, structures etc. present their frequency content below few hundreds hertz.
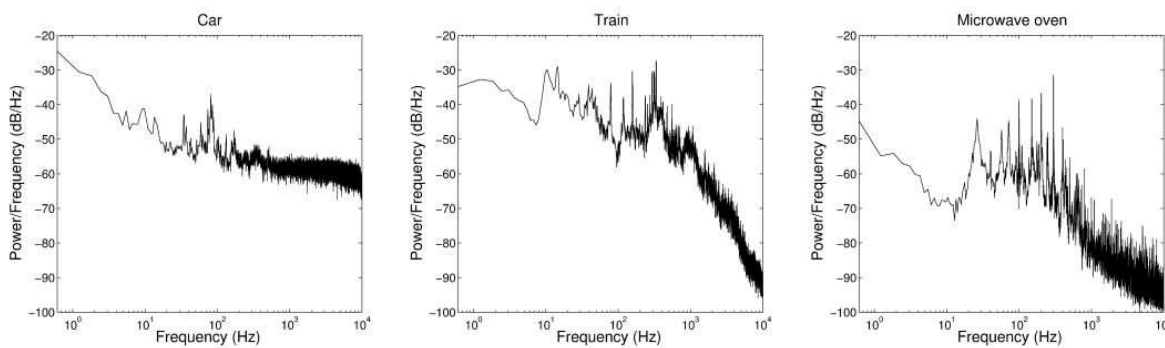

Figure 10. Vibration power spectra. Figure shows acceleration magnitudes (in db/Hz) vs frequency for three different environments.

As an example in Figure 10, three different spectra computed from vibrations taken from a car hood in motion, an operating microwave oven and a running train floor are presented.

All these different sources produce vibrations that are very large in amplitude and spectral characteristics. However, in these cases, like in great part of the cited examples, the ambient vibrations have their energy distributed over a wide frequency spectrum, with significant predominance of low frequency components and frequency tuning or a multimodal approach is not always possible due to geometrical/dynamical constraints. Hence, another frequency-robust solution for VEH is to 'transfer' the source vibration frequency to the harvester resonance frequency so that useful power can be harnessed in low frequency excitation scenarios.

A typical up-conversion schematic is presented in Figure 11, where the basic principle of such a device is evident [30]. The oscillator with elastic constant k has a resonant frequency in a lower region respect to the resonant frequencies of the piezoelectric beams. When the tooth passes and hits the cantilever tips, the cantilevers start oscillating at their natural frequency. Thus the low frequency vibration of the primary vibrating unit (i.e. the oscillating mass m) is transferred to the high frequency vibration of the secondary units (i.e. the piezoelectric

cantilevers). This provides a robust low frequency harvesting using high frequency structures as transduction elements.
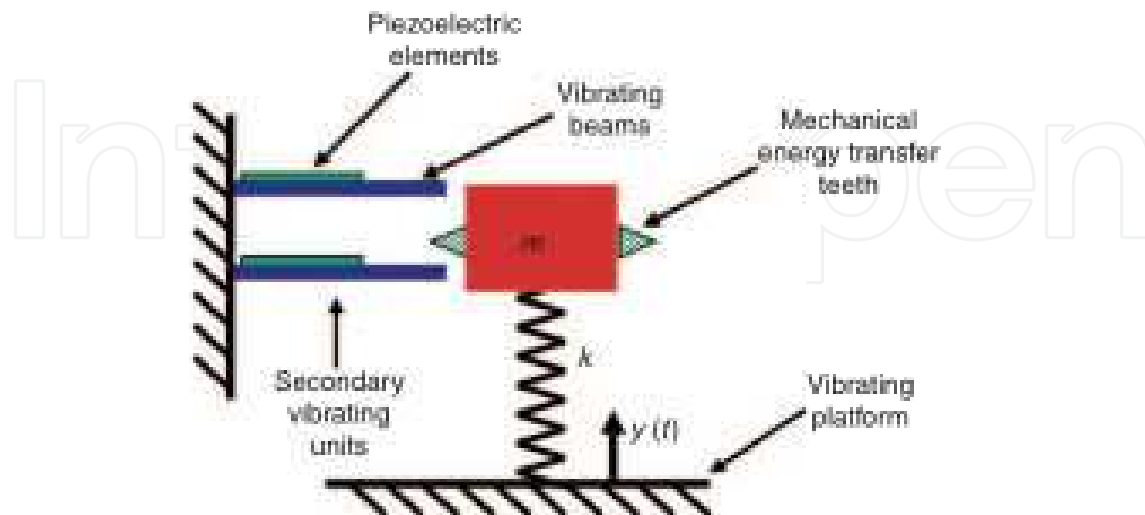

Figure 11. Schematic of an up-conversion VEH (source: Rastegar et al. 2006 [31]).

This frequency up-conversion technique was further pursued in few applications like the generators for low and variable speed rotary machineries [31]. It can be implemented combining different oscillators and interaction mechanisms, like magnetic or electrostatic, maintaining its basic principle.

This technique is a way to decouple the exciting frequency and the harvester vibration one, thus the performances are insensitive to the excitation frequency as long as it is less than the resonant frequency of the harvester. The drawback is that the 'first unit' resonance frequency needs to be tuned to the main frequency of the vibration source. In case the exciting vibrations are spread in a wide frequency range, the advantages of this method lose efficiency.

5. Non-linear techniques

All the above-mentioned strategies to harvest energy from the environment belong to the entire category of linear (or resonant) harvesting techniques. In general, for a generic linear system, even more complicated than a simple cantilever, the transfer function presents one or more peeks corresponding to the resonance frequencies and thus it is effective mainly when the incoming energy is abundant in that frequency region.

Unfortunately this is a serious limitation when it is required to build a vibration energy harvester of small dimension, for at least two main reasons, the first is that, as discussed above, the frequency spectrum of available vibrations instead of being sharply peaked at some frequency is usually very broad. The second reason is that the frequency spectrum of available

vibrations is particularly rich in energy in the low frequency range, and it is very difficult, if not impossible, to build small, low-frequency resonant systems.

Based on these considerations it is clear that vibration harvesters inspired by cantilever-like configurations present a number of drawbacks that limit seriously their field of application.

The optimal vibration harvester characteristics for a broadband response can be summarized in the following points:

- Resonant oscillators should be avoided. In fact a resonant oscillator is capable of harvesting energy only in a very narrow band, around its resonant frequency. Non-resonant oscillators have to be taken into account.

- Increase the capability of harvesting energy at low frequency (below few hundred Hz) because this is where most of the ambient energy is available. Due to geometrical constraints a small dimension linear harvester in not feasible.

- No need for frequency tuning after the initial set-up of the harvester. Frequency tuning is a feature of resonant systems, thus if we move to non-resonant systems this requirement will be automatically satisfied.

As we have seen before the search for the best solution in terms of non-resonant systems should start from the potential energy function *U(z)*. In fact *U(z)* plays the role of dynamical energy storage facility (before transduction) for our mechanical oscillator and thus it is here that we should focus our attention.

The best solution in terms of non-resonant systems should start from the potential energy function *U(z)*. In fact equation (1) can be rewritten as:

$$m\ddot{z} + d\dot{z} + \frac{dU(z)}{dz} + \alpha V = -m\ddot{y}, \tag{12}$$

where *U(z)* plays the role of dynamical energy storage facility (before transduction) for our mechanical oscillator and thus it is here that we should focus our attention.

To replace a linear oscillator with a non-linear one the condition is:

$$U(z) \neq \frac{1}{2}kz^2 \tag{13}$$

meaning oscillators whose potential energy is not quadratically dependent on the relevant displacement variable. In recent years few possible candidates have been explored [32-42] running from:

$$U(z) = az^{2n} \tag{14}$$

to other more complicated expressions.

For non-linear oscillators it is not possible to define a transfer function, like in paragraph (3.3), and thus a properly defined resonant frequency even if the power spectral density can show one or more well defined peeks for specific values of the frequencies.

In this section, two of these non-linear potential cases, will be briefly addressed.

5.1. Bistable cantilever

An interesting option for a nonlinear oscillator is to look for a potential energy that is multi-stable, instead of mono-stable (like the linear case, i.e. the harmonic potential). A particularly simple and instructive example on how to move from the linear (mono-stable) to a possible nonlinear (bi-stable) dynamics is represented by a slightly modified version of the vibration harvester cantilever analysed above (see Figure 12).
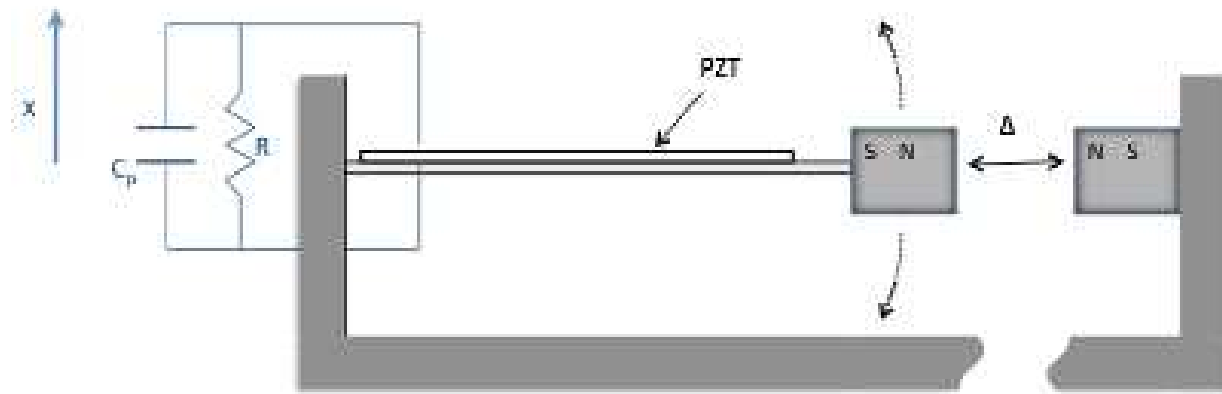

Figure 12. Schematic of the bi-stable energy harvester considered (source: Vocca et al., 2012 [32]).

This is a common cantilever with a bending piezoelectric layer. At the cantilever tip a small magnet is added. Under the action of the vibrating ground the pendulum oscillates alternatively bending the piezoelectric layer and thus generating a measurable voltage signal V. The dynamics of the inverted pendulum tip is controlled with the introduction of an external magnet conveniently placed at a certain distance Δ and with polarities opposed to those of the tip magnet. The interaction between the two magnets generates a force dependent from Δ that opposes the elastic restoring force of the bended beam. As a result, the inverted pendulum dynamics can show three different types of behaviours as a function of the distance Δ:

- when the two magnets are separated by a large distance ($\Delta \gg \Delta_0$) the inverted pendulum behaves like a linear oscillator. This situation accounts well for the usual operating condition analysed previously.

- If Δ is small ($\Delta \ll \Delta_0$) the pendulum is forced to oscillate at the left or at the right of the vertical. In the limit of small oscillations, this can still be described in terms of a linear oscillator but with a resonant frequency higher that in the previous case.

- In between the two previous cases it exists an intermediate condition ($\Delta=\Delta_0$) where the cantilever swings in a more complex way with small oscillations around each of the two equilibrium positions (left and right of the vertical) and large excursions from one to the other.

The nonlinear potential that can be considered in equation (12) is [32]:

$$U(z) = \frac{1}{2} k_e z^2 + (Az^2 + B\Delta^2)^{-\frac{3}{2}}$$

(15)

with k_e, A and B representing constants related to the physical parameters of the cantilever. Clearly when the distance Δ between the magnets grows very large the second term in (15) becomes negligible and the potential tends to the harmonic potential of the linear case, typical of the cantilever harvester.

In Figure 13 the potential $U(z)$ for the condition $\Delta=\Delta_0$ is shown. In this case the potential energy shows clearly two distinct equilibrium points separated by an energy barrier.
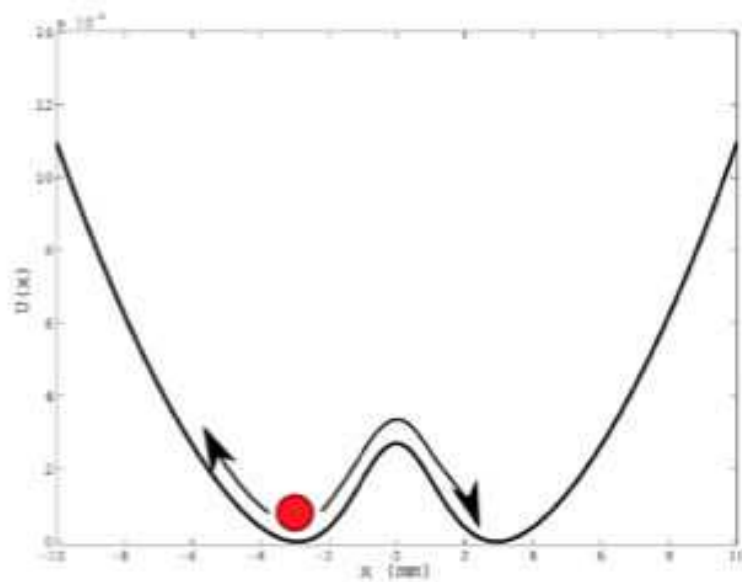

Figure 13. Potential energy $U(z)$ in (0.15) in arbitrary units when ($\Delta=\Delta_0$).

The overall qualitative behaviour is somehow summarized in Figure 14, where the average power ($P_{avg} = V_{rms}^2/R$) extracted from this vibration harvester is presented as a function of the distance parameter Δ. As it is well evident there is an optimal distance Δ_0) where the power peaks to a maximum [33]. Most importantly such a maximum condition is reached in a full nonlinear regime (bistable condition of the potential) resulting larger (at least a factor 4) than the value in the linear condition (far right in Figure 14).
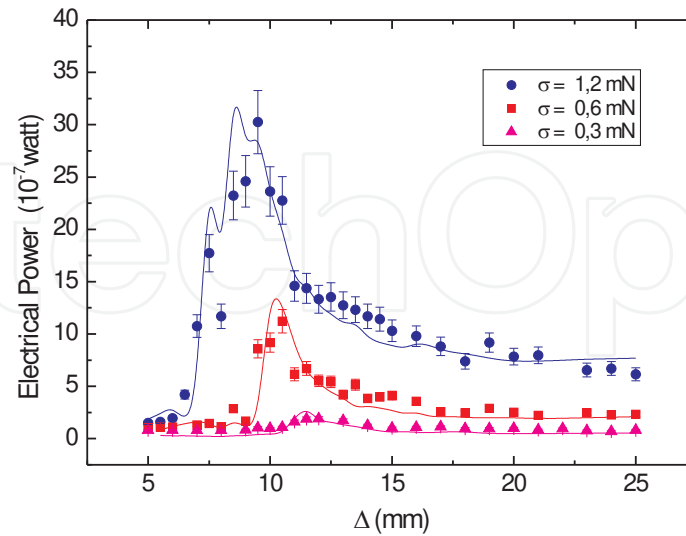
Figure 14. Piezoelectric nonlinear vibration harvester mean electrical power ($P_{avg}=V_{rms}^2/R$) as a function of the distance Δ between the two magnets (source: Cottone et al. 2009 [33]]).

5.2. Buckled beam

Buckled beams represent other possible structures to implement nonlinear VEH. In particular considering a piezoelectric beam clamped on both ends on a base excited vertically, it has demonstrated by Cottone et al.[33], that if the beam is subjected to a compression along his longitudinal axis (see Figure 15) the harvested power increases if the beam is vibrationally excited by a random noise.
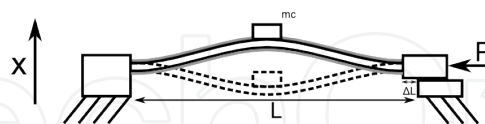

Figure 15. Schematic of a piezoelectric buckled beam (source: Vocca et al. 2013 [34]).

The equations that link the beam motion to the output voltage across a resistive load R_L are the followings [35]:

$$m\ddot{x} + \gamma\dot{x} + k_3 x^3 + (k_2 - k_1 V)x + k_0 V = \sigma\xi, \tag{16}$$

$$\frac{1}{2}C\dot{V} + \frac{V}{R_L} = -k_1 x\dot{x} + k_0\dot{x} \tag{17}$$

where m, γ, C and R_L are the equivalent mass, the viscous parameter, the coupling capacitance and the resistive load respectively. The term k_3 is the beam third order stiffness coefficient; k_0 and k_1 are the piezoelectric coupling terms due to the bending and to the axial strain of the beam respectively. The term $k_2 = k_a - k_b \Delta L$ is the stiffness parameter, where k_a and k_b are constants depending on physical parameters of the beam. When the beam is compressed by increasing ΔL (or equivalently the lateral load P), the stiffness becomes negative and the system becomes bistable. The buckled model in equation (16) is valid for small compressions ΔL. The $\sigma \xi(t)$ represents the vibration force that drives the beam.

It has been demonstrated in [34], that considering as excitation a random force with a Gaussian distribution, zero mean and exponentially auto-correlated, the output power that represents the amount of the energy harvested per second, increases increasing ΔL. In Figure 16 the average electrical power versus the compression length ratio respectively for the experimental (on the left) and numerical models (on the right) are shown for three noise amplitudes.
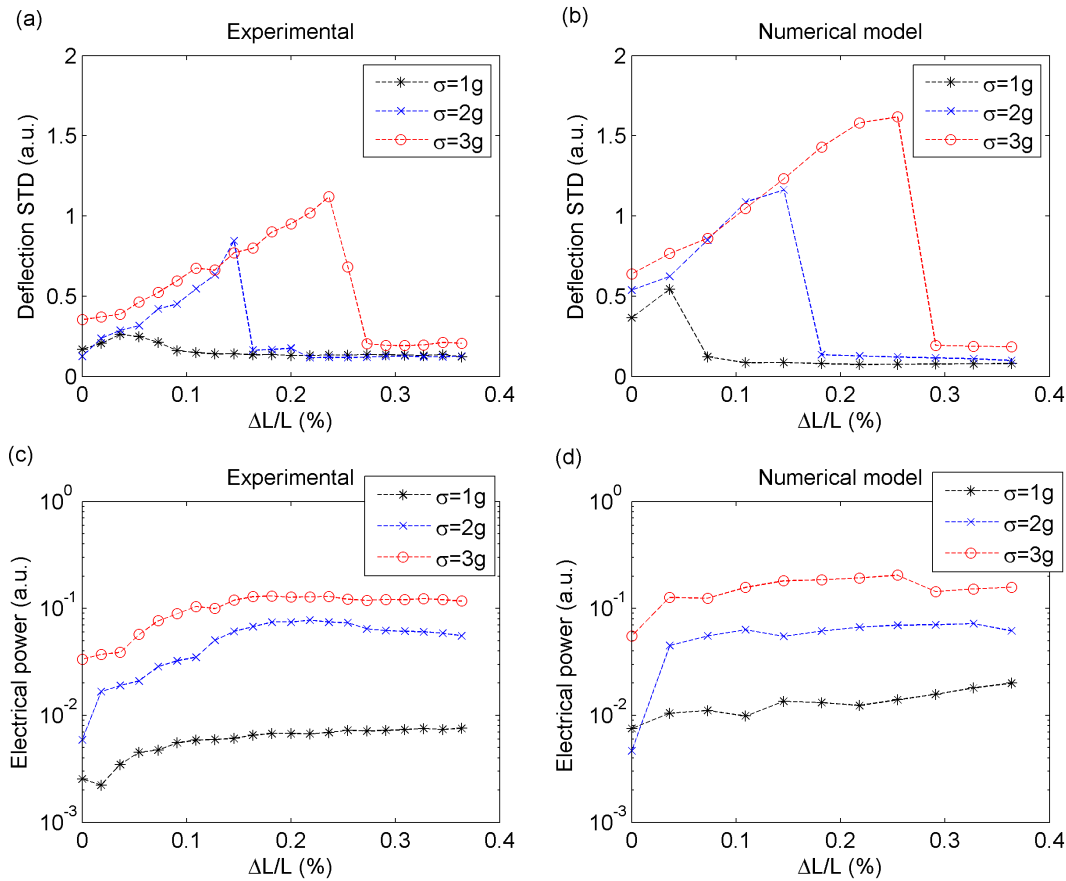

Figure 16. Electrical average power versus relative compression $\Delta L/L$ (%) for experiment (left column) and numerical simulation (right column). (Source: Cottone et al. 2012, [34]).

Moreover, the piezoelectric beam produces up to an order of magnitude more electric power when it is compressed than in the unbuckled case.

5.3. Comparison of the two methods

In Vocca et al. [34] as a comparison between the cantilever nonlinear configuration and the buckled beam, the same piezoelectric element subjected to a fixed vibrating body in both configurations has been simulated. The piezoelectric oscillators output responses obtained as a function of the nonlinear parameter are compared in Figure 17.
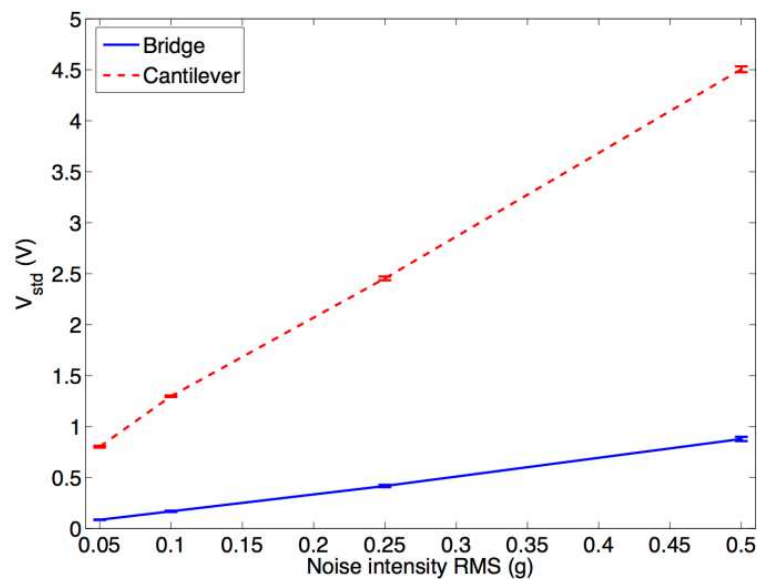

Figure 17. Comparison between cantilever and buckled beam response as a function of the noise intensity (source: Vocca et al. 2013, [35]).

The cantilever configuration appears to perform better than the beam in all the conditions. Although the buckled beam configuration is an interesting option for an harvester configuration where the introduction of a magnetic field is undesirable, generally it becomes evident that the cantilever harvester configuration is the best choice once in presence of an exponentially correlated noise.

6. Conclusions

In this chapter we have discussed the various strategies developed for vibration energy harvesting. A specific reference to the role of linearity and nonlinearity has been discussed. We have shown that linear resonant systems are clearly limited in their practical applications even if various techniques have been developed to increase the bandwidth. It has been shown that more complex VEHs based on non-linear mechanical oscillators can outperform them in a number of realistic energy harvesting scenarios. In fact, from comparative works that have been recently published it comes out that nonlinear monostable and bistable structures are the best opinion for enhancing the overall performances and improving the flexibility of vibration powered electronics. [35]

Author details

Helios Vocca[1] and Francesco Cottone[2]

1 NiPS Laboratory, Department of Physics, University of Perugia, Perugia, INFN Perugia and Wisepower srl, Italy

2 ESIEE Paris, University of Paris Est, Paris, France

References

[1] C. S. Raghavendra, *et al.*, *Wireless sensor networks*: Springer, 2006.

[2] N. Gershenfeld, *et al.*, "The Internet of things," *Scientific American,* vol. 291, pp. 76-81, 2004.

[3] P. D. Mitcheson, *et al.*, "Energy harvesting from human and machine motion for wireless electronic devices," *Proceedings of the IEEE,* vol. 96, pp. 1457-1486, 2008.

[4] A. Bilbao, *et al.*, "Ultra-low power wireless sensing for long-term structural health monitoring," 2011, p. 798109.

[5] K. Cook-Chennault, *et al.*, "Powering MEMS portable devices—a review of non-regenerative and regenerative power supply systems with special emphasis on piezoelectric energy harvesting systems," *Smart materials and structures,* vol. 17, p. 043001, 2008.

[6] L. Wang and F. Yuan, "Energy harvesting by magnetostrictive material (MsM) for powering wireless sensors in SHM," 2007, pp. 18-22.

[7] T. Ikeda, *Fundamentals of Piezoelectricity*. Walton St, Oxford, UK: Oxford University Press 1996.

[8] A. b. E. Lefeuvre, C. Richard, L. Petit, D. Guyomar, "A comparison between several approaches of piezoelectric energy harvesting," *J. Phys. IV France,* vol. 128, pp. 177-186, 2005.

[9] T. G. McKay, *et al.*, "Soft generators using dielectric elastomers," *Applied Physics Letters,* vol. 98, pp. 142903-142903-3, 2011.

[10] G. Poulin, *et al.*, "Generation of electrical energy for portable devices Comparative study of an electromagnetic and a piezoelectric system," *Sensors & Actuators: A. Physical,* vol. 116, pp. 461-471, 2004.

[11] S. P. Beeby, *et al.*, "A micro electromagnetic generator for vibration energy harvesting," *Journal of Micromechanics and Microengineering,* vol. 17, p. 1257, 2007.

[12] P. Wang, *et al.*, "A micro electromagnetic low level vibration energy harvester based on MEMS technology," *Microsystem Technologies*, vol. 15, pp. 941-951, 2009.

[13] I. Sari, *et al.*, "An electromagnetic micro power generator for wideband environmental vibrations," *Sensors and Actuators A: Physical*, vol. 145, pp. 405-413, 2008.

[14] S. Meninger, *et al.*, "Vibration-to-electric energy conversion," *Very Large Scale Integration (VLSI) Systems, IEEE Transactions on*, vol. 9, pp. 64-76, 2001.

[15] F. Peano and T. Tambosso, "Design and optimization of a MEMS electret-based capacitive energy scavenger," *Microelectromechanical Systems, Journal of*, vol. 14, pp. 429-435, 2005.

[16] P. Basset, *et al.*, "A batch-fabricated and electret-free silicon electrostatic vibration energy harvester," *Journal of Micromechanics and Microengineering*, vol. 19, p. 115025, 2009.

[17] S. Roundy, *et al.*, "MICRO-ELECTROSTATIC VIBRATION-TO-ELECTRICITY CONVERTERS," *Fuel Cells (methanol)*, vol. 220, p. 22.

[18] P. Miao, *et al.*, "MEMS inertial power generators for biomedical applications," *Microsystem Technologies*, vol. 12, pp. 1079-1083, 2006.

[19] X. Chen, *et al.*, "1.6 V nanogenerator for mechanical energy harvesting using PZT nanofibers," *Nano letters*, vol. 10, pp. 2133-2137, 2010.

[20] X. Wang, *et al.*, "Direct-Current Nanogenerator Driven by Ultrasonic Waves," *Science*, vol. 316, p. 102, 2007.

[21] C. B. Williams and R. B. Yates, "Analysis Of A Micro-electric Generator For Microsystems," *Solid-State Sensors and Actuators, 1995 and Eurosensors IX. Transducers' 95. The 8th International Conference on*, vol. 1, 1995.

[22] S. Roundy, *et al.*, *Energy Scavenging For Wireless Sensor Networks with special focus on Vibrations*: Kluwer Academic Publisher, 2004.

[23] G. Sebald, *et al.*, "Experimental Duffing oscillator for broadband piezoelectric energy harvesting," *Smart materials and structures*, vol. 20, p. 102001, 2011.

[24] L. Tang, *et al.*, "Toward broadband vibration-based energy harvesting," *Journal of Intelligent Material Systems and Structures*, vol. 21, pp. 1867-1897, 2010.

[25] S. Roundy and Y. Zhang, "Toward self-tuning adaptive vibration-based microgenerators," in *Proc. SPIE*, 2004, pp. 373-384.

[26] X. Wu, *et al.*, "A frequency adjustable vibration energy harvester," *Proceedings of PowerMEMS*, pp. 245-248, 2008.

[27] V. R. Challa, *et al.*, "A coupled piezoelectric–electromagnetic energy harvesting technique for achieving increased power output through damping matching," *Smart materials and structures*, vol. 18, p. 095029, 2009.

[28] Y. Tadesse, *et al.*, "Multimodal energy harvesting system: piezoelectric and electro-magnetic," *Journal of Intelligent Material Systems and Structures,* vol. 20, pp. 625-632, 2009.

[29] S. Shahruz, "Design of mechanical band-pass filters for energy scavenging," *Journal of Sound and Vibration,* vol. 292, pp. 987-998, 2006.

[30] M. Ferrari, *et al.*, "Piezoelectric multifrequency energy converter for power harvesting in autonomous microsystems," *Sensors and Actuators A: Physical,* vol. 142, pp. 329-335, 2008.

[31] J. Rastegar, *et al.*, "Piezoelectric-based power sources for harvesting energy from platforms with low frequency vibration," in *Proc. SPIE,* 2006, p. 617101.

[32] H. Vocca, *et al.*, "Kinetic energy harvesting with bistable oscillators," *Applied Energy,* 2012.

[33] F. Cottone, *et al.*, "Nonlinear energy harvesting," *Physical Review Letters,* vol. 102, 2009.

[34] F. Cottone, *et al.*, "Piezoelectric buckled beams for random vibration energy harvesting," *Smart materials and structures,* vol. 21, 2012.

[35] H. Vocca, *et al.*, "A comparison between nonlinear cantilever and buckled beam for energy harvesting," *European Physical Journal,* 2013.

[36] L. Gammaitoni, *et al.*, "Nonlinear oscillators for vibration energy harvesting," *Applied Physics Letters,* vol. 94, pp. 164102-164102-3, 2009.

[37] L. Gammaitoni, *et al.*, "The benefits of noise and nonlinearity: Extracting energy from random vibrations," *Chemical Physics,* vol. 375, pp. 435-438, 2010.

[38] M. Ferrari, *et al.*, "Improved energy harvesting from wideband vibrations by nonlinear piezoelectric converters," *Sensors and Actuators A: Physical,* 2010.

[39] A. Arrieta, *et al.*, "A piezoelectric bistable plate for nonlinear broadband energy harvesting," *Applied Physics Letters,* vol. 97, p. 104102, 2010.

[40] B. Andò, *et al.*, "Nonlinear mechanism in MEMS devices for energy harvesting applications," *Journal of Micromechanics and Microengineering,* vol. 20, p. 125020, 2010.

[41] D. A. Barton, *et al.*, "Energy harvesting from vibrations with a nonlinear oscillator," *Journal of vibration and acoustics,* vol. 132, 2010.

[42] S. C. Stanton, *et al.*, "Nonlinear dynamics for broadband energy harvesting: Investigation of a bistable piezoelectric inertial generator," *Physica D: Nonlinear Phenomena,* vol. 239, pp. 640-653, 2010.